The Difference Between Stiffness and Quasi-Stiffness in the Context of Biomechanical Modeling

Elliott J. Rouse*, *Member, IEEE*, Robert D. Gregg, *Member, IEEE*, Levi J. Hargrove, *Member, IEEE*, and Jonathon W. Sensinger, *Member, IEEE*

***Abstract*—The ankle contributes the majority of mechanical power during walking and is a frequently studied joint in biomechanics. Specifically, researchers have extensively investigated the torque–angle relationship for the ankle during dynamic tasks, such as walking and running. The slope of this relationship has been termed the "quasi-stiffness." However, over time, researchers have begun to interchange the concepts of quasi-stiffness and stiffness. This is an especially important distinction as researchers currently begin to investigate the appropriate control systems for recently developed powered prosthetic legs. The quasi-stiffness and stiffness are distinct concepts in the context of powered joints, and are equivalent in the context of passive joints. The purpose of this paper is to demonstrate the difference between the stiffness and quasi-stiffness using a simple impedance-controlled inverted pendulum model and a more sophisticated biped walking model, each with the ability to modify the trajectory of an impedance controller's equilibrium angle position. In both cases, stiffness values are specified by the controller and the quasi-stiffness are shown during a single step. Both models have widely varying quasi-stiffness but each have a single stiffness value. Therefore, from this simple modeling approach, the differences and similarities between these two concepts are elucidated.**

***Index Terms*—Ankle impedance, biped model, inverted pendulum, prosthetics, quasi-stiffness, stiffness.**

I. Introduction

THE relationship between joint angle and torque is a frequently studied concept in biomechanics with numerous applications, including motor control, prosthesis/orthosis design, and biologically inspired robotics [1]–[4]. This relationship is particularly important at the ankle, which contributes the majority of mechanical power during walking [5]. Loss of this joint significantly impairs gait attributes, resulting in 11–40% slower self-selected walking speeds and increases in metabolic expenditures of 10–60% during walking [6]–[8]. These deficits are especially relevant as 130 000 lower limb amputations occur annually [9], and injuries from overseas conflicts have further increased these numbers. Although powered ankle prostheses have recently been developed [4], [10], appropriate biomimetic mechanical properties are unknown. Additionally, inconsistencies in terminology must be resolved in order to prevent misconceptions regarding the true mechanical properties of the ankle and to promote the development of biomimetic control systems for powered ankle prostheses.

The ankle torque–angle relationship has typically been studied during performance of a specific task such as walking or running. In these cases, the derivative of the torque–angle relationship with respect to angle is known as the *quasi-stiffness*. The distinction between quasi-stiffness and stiffness was discussed by Latash and Zatsiorsky [3], wherein the authors stressed the important energy-storing nature of stiffness and discussed physiological joint structures and their contribution to mechanical properties. The joint *stiffness* can be defined as the position-dependent component that stores (and releases) energy.

Hansen *et al*. published ankle torque–angle relationships for various walking speeds, noting that quasi-stiffness characteristics of the human ankle appear to change as walking speed increases. Interestingly, the torque–angle relationship was approximately linear for the majority of stance phase at normal walking speeds. This suggested that the appropriate ankle quasi-stiffness could be obtained by using a single passive spring element that could serve as the benchmark for passive ankle prosthesis design. Subsequently, quasi-stiffness has been investigated with respect to walking while bearing loads [11] and as a postsurgical research metric [12].

However, the quasi-stiffness of human gait must be interpreted carefully. Studies on human hopping and running have investigated the spring stiffness required to replicate modeled movements and determined that ankle stiffness is a major contributor to overall leg stiffness during human hopping [13]. Furthermore, Davis and DeLuca [18] analyzed "dynamic ankle stiffness" during walking by investigating the quasi-stiffness in healthy subjects and in subjects with cerebral palsy. However, since the ankle and knee are capable of doing positive work, quasi-stiffness is a description of the dynamic task in the

Manuscript received June 21, 2012; revised September 12, 2012; accepted November 11, 2012. Date of publication November 29, 2012; date of current version January 16, 2013. This work was supported by the U.S. Army Telemedicine and Advanced Technology Research Center under Award W81XWH-09-2-0020, the National Institute of Neurological Disorders and Stroke under Award F31NS074687, and the Rice Foundation. *Asterisk indicates corresponding author.*

*E. J. Rouse is with the Department of Biomedical Engineering, Northwestern University, Evanston, IL 60208 USA, with the Center for Bionic Medicine, Rehabilitation Institute of Chicago, Chicago, IL 60611 USA (e-mail: e-rouse@u.northwestern.edu).

R. D. Gregg is with the Center for Bionic Medicine, Rehabilitation Institute of Chicago, Chicago, IL 60611 USA, and also with the Department of Mechanical Engineering, Northwestern University, Evanston, IL 60208 USA (e-mail: rgregg@ieee.org).

L. J. Hargrove and J. W. Sensinger are with the Department of Physical Medicine and Rehabilitation, Northwestern University, Evanston, IL 60208 USA, and also with the Center for Bionic Medicine, Rehabilitation Institute of Chicago, Chicago, IL 60611 USA (e-mail: l-hargrove@northwestern.edu; sensinger@ieee.org).

Color versions of one or more of the figures in this paper are available online at http://ieeexplore.ieee.org.

Digital Object Identifier 10.1109/TBME.2012.2230261

torque–angle domain, rather than a representation of stiffness or impedance. Hence, a shift in the terminology may be required as research expands into the development of biomimetic prosthesis control systems.

Currently, the concepts of quasi-stiffness and stiffness are used interchangeably [13]–[18]. However, quasi-stiffness and stiffness are distinct concepts, except when the joint is constrained to be passive. It is important to delineate this distinction because powered ankle prostheses actively change their rendered stiffness and equilibrium positions, providing an endless combination of stiffness and quasi-stiffness values that alter how the device interacts with its user. Before we can achieve biomimetic control of these devices, we must thoroughly understand ankle quasi-stiffness and stiffness, and their relation to each other. Additionally, this understanding may elucidate properties of ankle spasticity—i.e., the altered joint mechanics that result from upper motor neuron syndrome [19].

In this study, we demonstrate differences between ankle quasi-stiffness and stiffness using two computational models with force information that could be obtained in a standard laboratory setting. Initially, we consider a simulated inverted pendulum with an impedance-controlled motor at the base. The impedance controller's equilibrium position trajectory is varied in order to demonstrate the sensitivity of quasi-stiffness to this input and the wide range of quasi-stiffness values that can be observed. This model builds on Latash's inverted pendulum illustration [3] by adding a controller "stiffness" term to highlight how stiffness may differ from the quasi-stiffness. We then present a novel computational walking model incorporating an impedance controller at the ankle, which produces a torque–angle relationship similar to that determined in human studies, to demonstrate that the quasi-stiffness is similarly sensitive under dynamic conditions. In this paper, the controller stiffness is a metaphor, since there is no actual energy storage element—it simply represents what would be possible from a stable controller that can add/remove energy.

II. Inverted Pendulum Model

A. Methods

Human standing and walking are frequently approximated using an inverted pendulum model [20], [21]. This study incorporates an impedance-controlled, ideal motor at the pendulum base that is capable of adding energy into the system. For our purposes, the motor's impedance will be limited to a constant stiffness with a time-varying equilibrium position. Alternatively, a time-varying stiffness function could have been chosen to simulate behavior that requires addition/subtraction of energy; however, for simplicity, only the equilibrium position was allowed to vary. Thus, the equation of motion governing the pendulum is

$$I\ddot{\theta} = k_a\left(\theta - \theta_d\left(t\right)\right) - WL\sin\left(\theta\right) \tag{1}$$

where I is the inertia, k_a is the stiffness of the impedance controller, θ is the pendulum angle, $\theta_d(t)$ is the equilibrium position as a function of time, L is the length of the massless rod, and W is the pendulum weight (see Fig. 1). The right-hand side of (1) denotes net torque about the base and dictates pendulum dynamics. The reaction torque about the base will be the torque component from the motor; this information was acquired in our simulations and is similar to the force platform information typically acquired in a laboratory setting, yielding forces and center of pressure (COP).

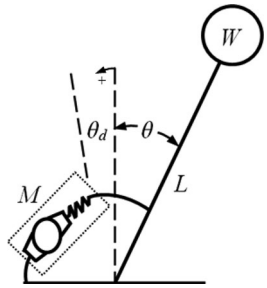

Fig. 1. Model of the inverted pendulum shown with motor M and pendulum weight W. Motor impedance control system shown with imposed controller stiffness represented as a physical spring.

The inverted pendulum simulation was constructed in Simulink (The Mathworks, Natick MA). Inputs included the initial conditions for position and velocity and the equilibrium position trajectory; outputs included the reaction torque about the base and the pendulum angle. The simulation lasted 0.5 s and quasi-stiffness values were approximated from the numerical derivative of the torque–angle function. The mass was 80 kg, the length L was 1 m—to approximate able-bodied gait—and the stiffness of the motor's impedance controller was 10 N·m/rad/kg—a value commonly seen in passive prosthetic ankles and greater than the inherent small-angle destabilizing torque caused by gravity.

Three cases were tested: the equilibrium position trajectory was either 1) a constant value; 2) the solution of the differential equation with purely gravitational mechanics (i.e., unperturbed hinge-like rotation); or 3) a sine wave with amplitude of 0.35 rad and a frequency of 0.5 Hz. The constant equilibrium position was 0.17 rad. The initial condition for the pendulum angle was 0.09 rad with an angular velocity of zero.

B. Results

Case 1: The system behaved passively, yielding a quasi-stiffness that matched the stiffness of the motor's impedance controller [10 N·m/rad/kg, Fig. 2(a)].

Case 2: The difference between the actual and equilibrium positions was always zero. This resulted in no reaction torque at the base and acceleration of the pendulum due to the net torque of gravity. With zero reaction torque, the derivative of the torque–angle function was zero [see Fig. 2(b)].

Case 3: The pendulum angle was outpaced by the equilibrium position, creating a negative relationship between the torque and the angle [see Fig. 2(c)] leading to negative quasi-stiffness values—ranging from -8580 to -140 N·m/rad/kg—which are not physically realizable with a spring.

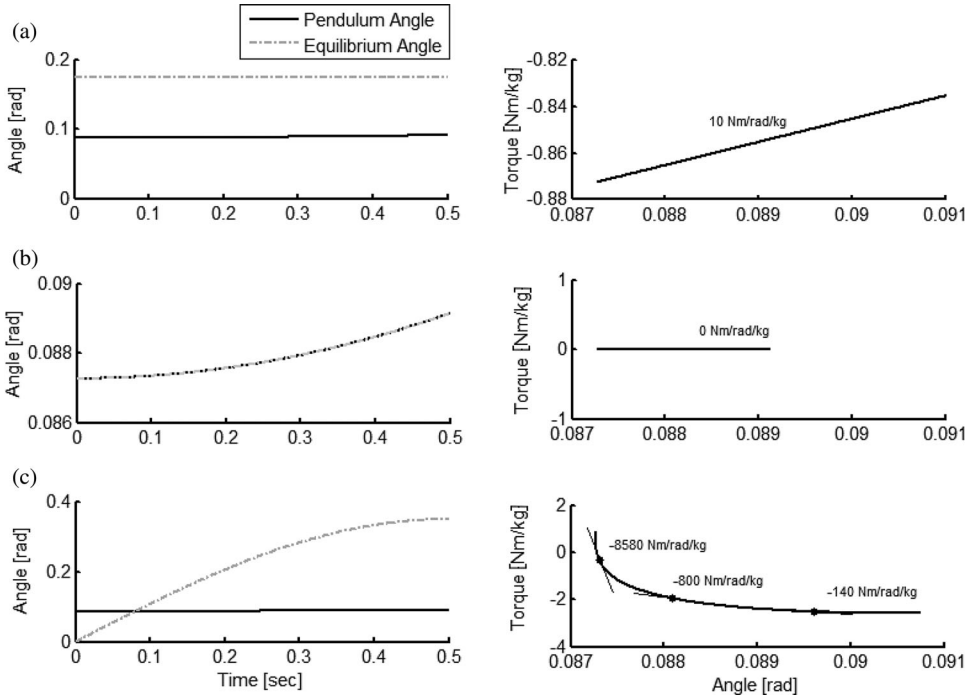

Fig. 2. Pendulum angle (black) and equilibrium angle (gray) are shown as a function of time (left) and the torque as a function of angle (right) for (a) case 1, (b) case 2, and (c) case 3. The quasi-stiffness values are given for each case and the mechanical stiffness is 10 N·m/rad/kg.

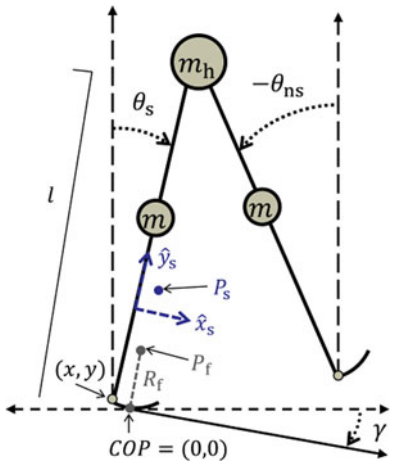

Fig. 3. Diagram of a biped model. The origin of the shank coordinate frame (dashed axes) is drawn above the ankle for clarity but is actually modeled to coincide with the ankle joint (located at the heel for simplicity).

III. Biped Model

A. Methods

The planar biped (see Fig. 3) has one hip joint and constant-curvature rocker feet connected to ankle joints. We model this biped as a kinematic chain attached to the COP—the point on the plantar sole where the resultant ground reaction force is imparted. The configuration vector of this model is given by $q = (x, y, \theta_s, \theta_{\rm ns})^T$, where x and y are the Cartesian coordinates of the ankle center (for simplicity the ankle is located at the heel) with respect to the COP (defined at the origin), and θ_s and $\theta_{\rm ns}$ are the respective angles of the stance and nonstance/swing legs with respect to vertical.

The biped's dynamics are continuous during single-support phase until the swing foot contacts the ground, which initiates the double-support transition into the next step cycle. We define a function $h_\gamma(q)$ to give the heel height of the swing foot with slope angle γ, so heel strike occurs when $h_\gamma(q) = 0$. The double-support transition is modeled as an instantaneous impact event with a perfectly plastic (inelastic) collision [22]. The joint trajectory is therefore subjected to the discontinuous impact map Δ (which also switches the values of θ_s and $\theta_{\rm ns}$ to model the change in stance/swing legs) in the hybrid dynamical system

$$M(q)\ddot{q} + C(q,\dot{q})\dot{q} + G(q) + A^T(q)\lambda = \tau \quad \text{for } h_\gamma(q) > 0$$
$$\left(q^+, \dot{q}^+\right) = \Delta(q^-, \dot{q}^-) \quad \text{for } h_\gamma(q) = 0$$

where $(^+)$ denotes the postimpact and $(^-)$ the preimpact state, M is the inertia/mass matrix, C contains the Coriolis/centrifugal terms, G is the vector of gravitational torques, A is the constraint vector corresponding to rocker foot motion, λ is the Lagrange multiplier (producing the forces needed to enforce the foot constraint), and τ is the vector of external torques from muscles/actuators. This dynamical modeling approach is described in more detail in [23].

1) Rocker Foot Constraint: We model the rocker foot by constraining the heel point (x, y) to an arc that has radius $R_{\rm f}$ and intersects the COP. The center of rotation $P_{\rm f}$ is defined in a moving reference frame such that the vector between $P_{\rm f}$ and the COP is always normal to the ground with radius $\|{\rm COP} - P_{\rm f}\| = R_{\rm f}$. This constraint can be given in model coordinates by an equation $b(q) = 0$ [24]. Following the method of [25], we derive constraint vector $A = \frac{\partial b}{\partial q}$ and Lagrange multiplier λ.

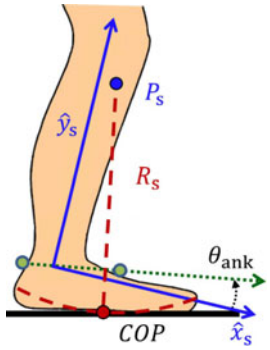

Fig. 4. Effective shape (dashed red curve) with a radius of curvature R_s. The center of rotation is a point P_s, which is constant in the shank coordinate frame (solid axes). Note that the relative ankle angle θ_{ank} is shown instead of the global leg angle θ_s.

2) Ankle Control Strategy: This model has passive walking gaits ($\tau = 0$) down shallow slopes for certain model parameters (where the kinetic energy dissipated at impact equals the potential energy introduced along the decline slope [22]), but we are interested in how ankle actuation influences the quasi-stiffness during locomotion. We model actuation only at the ankle by defining vector $\tau = Bu$, where $B = [0, 0, 1, 0]^T$ maps the scalar ankle torque u into the biped's coordinate system. The ankle has a rotary spring damper (with stiffness K_p and viscosity K_d) in series with an actuator that can continuously change the spring equilibrium angle θ_s^{des}, so the ankle torque is given by $u = -K_p(\theta_s - \theta_s^{\mathrm{des}}) - K_d(\dot{\theta}_s - \dot{\theta}_s^{\mathrm{des}})$. We define a desired ankle trajectory from the *effective shape* of the human ankle–foot complex during walking [26]. This shape, which resembles a circular arc (see Fig. 4), characterizes how the ankle joint moves as the COP travels from heel to toe during single-support phase.

The effective shape is the trajectory of the COP mapped into a shank-based reference frame (axes $\hat{x}_s, \hat{y}_s$ in Figs. 3 and 4). This trajectory has constant curvature with radius R_s about the center of rotation P_s, which is constant in the shank coordinate frame. We can then model the desired effective shape as a kinematic constraint $\|\mathrm{COP} - P_s\| = R_s$, wherein the COP reference frame P_s depends on the ankle angle. The desired kinematic constraint is then automatically satisfied during heel contact (when $x = y = 0$); the ankle provides zero torque until the foot begins to roll. When $x > 0$, we can solve the desired kinematic constraint for $\theta_s = f(x, y)$, where the mapping f from COP location to stance leg angle depends on constants R_s and P_s. The x-component of the COP evolves monotonically (i.e., nondecreasing) over a steady stance cycle, so in this control strategy the COP serves as a phase variable that drives the progression of ankle kinematics by $\theta_s^{\mathrm{des}} = f(x, y)$. More detail on this control approach can be found in [24] and [27].

B. Results

We chose the model parameters shown in Table I based on adult (male) means reported by de Leva [28], grouping the trunk masses at the hip. The rocker foot radius was set to three-tenths of leg length, which is typical of human foot compliance [29].

TABLE I
MODELING AND CONTROL PARAMETERS

Parameter	Variable	Value
Hip mass	m_h	31.73 kg
Leg mass	m	13.5 kg
Leg length	l	0.856 m
Slope angle	γ	0.01 rad
Foot radius	R_f	0.26 m
Effective radius	R_s	0.45 m
Effective center	P_s	(0.005, 0.45) m
Ankle stiffness	K_p	6 Nm/rad/kg
Ankle viscosity	K_d	0.19 Nm-s/rad/kg

Since passive gaits typically comprise short steps, we obtained natural step lengths by adopting a larger effective radius of 0.45 m. We chose a stiffness of 6 N·m/rad/kg based on measurements of the human ankle [30] and a viscosity that provides a damping ratio of 0.3 [31]. The center of rotation P_s of the effective shape is adopted from [1].

We simulated this biped in MATLAB (The Mathworks) and found stable walking gaits on a slope of $\gamma = 0.01$ rad using the methods described in [24]. Recall that we have defined the stance leg angle with respect to vertical, which is often called the global tibia angle. The more commonly studied ankle angle, defined between the shank and foot (see Fig. 4), was obtained from our coordinates by $\theta_{\mathrm{ank}} = 2\sin^{-1}(\frac{\sqrt{x^2+y^2}}{2R_f}) + \gamma - \theta_s$ and used to show the torque–angle relationship in Fig. 5.

The quasi-stiffness (i.e., the tangential slope) in Fig. 5(b) only briefly passes through the actual stiffness of 6 N·m/rad/kg—most quasi-stiffness values do not resemble the mechanical stiffness of the ankle. At the beginning of the stance cycle, the quasi-stiffness is approximately zero, because the actual leg angle is equal to the desired angle after heel strike and the ankle controller does not produce corrective torques. The overall trend in quasi-stiffness values—from zero after ipsilateral heel strike, to positive, to negative, and then to infinity near contralateral heel strike—is consistent with human walking at normal speeds as seen in the torque–angle plots of [1]. The fact that we produced similar regions of quasi-stiffness values—the vast majority not matching the model's mechanical stiffness—demonstrates that human ankle mechanics may also not be well represented by quasi-stiffness measurements.

IV. Discussion

Quasi-stiffness is the derivative of the experimentally determined torque–angle relationship and has been extensively studied over the past several decades. More recently, many authors have begun to use the terms stiffness and quasi-stiffness interchangeably when describing human joint dynamics. To provide clarity, this study demonstrates the difference between stiffness and quasi-stiffness from the perspective of biomechanical modeling. The differences between these concepts may become increasingly important as biomimetic control systems are developed for powered prosthetic ankles.

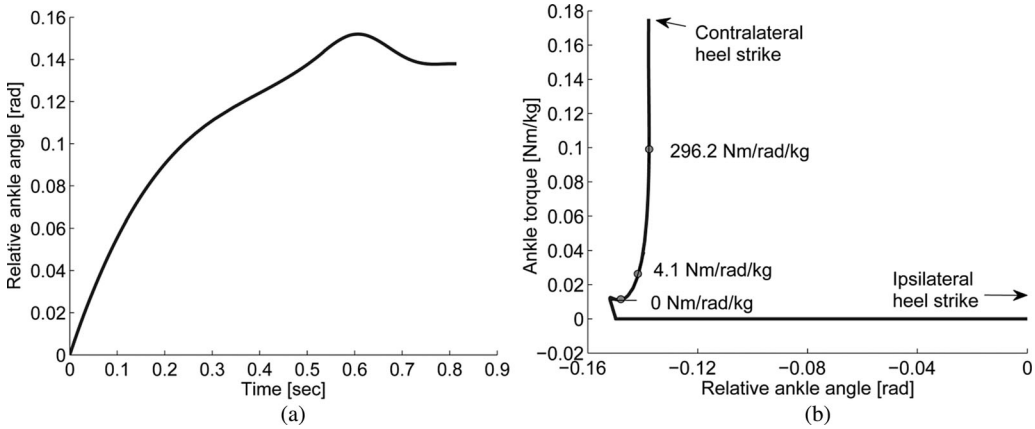

Fig. 5. (a) Relative ankle angle trajectory over time. (b) Ankle torque–angle plot (of the non-zero region) during simulated walking. Quasi-stiffness values (i.e., tangential slopes) are shown at points along the curve. Note that the mechanical stiffness is 6 N·m/rad/kg.

Using a simple impedance-controlled inverted pendulum model, quasi-stiffness values were determined for varying controller equilibrium position trajectories. Three cases were investigated: when the equilibrium position trajectory 1) was held constant at 0.17 rad; 2) was dictated by passive rotation; and 3) followed a 0.35 rad, 0.5 Hz sine wave. These three cases were chosen because they demonstrate the sensitivity of quasi-stiffness to the specifications of a controller that is capable of doing positive work.

When the controller had a constant equilibrium position trajectory, the movement of the pendulum toward the equilibrium position translated directly into a proportional reaction torque at the base, yielding a quasi-stiffness equal to the controller's stiffness. Thus, the quasi-stiffness is mechanically equivalent to the controller stiffness when the system is behaving with passive dynamics. In this case, the simulated measurements were made during a dynamic movement, not in equilibrium—since the equilibrium angle was invariant, energy was stored in the passive joint and is returned to the model. This scenario demonstrates that the term quasi-stiffness is more appropriate for describing a powered system in terms of the passive dynamics that replicate the specific task, rather than for describing a passive system. That is, when the dynamics are passive, the term "stiffness" already adequately describes the torque–angle relationship, and the modifier "quasi" is unnecessary.

When the equilibrium position trajectory was equivalent to hinge-like rotation, the reaction torque was zero because the angle did not diverge from the equilibrium position trajectory that was governed by gravitational mechanics. This yielded a quasi-stiffness value of zero throughout; however, the stiffness of the impedance-controlled pendulum was 10 N·m/rad/kg. Any interaction with the pendulum would displace it from the equilibrium position trajectory and it would render the controller stiffness.

When the controller's equilibrium position trajectory was altered, we see a dramatic effect; the equilibrium position began at zero and increased to approximately 0.31 rad, while the pendulum angle began at 0.087 rad and tended to approximately 0.090 rad. During the simulation, the pendulum angle approached the equilibrium position; however, the equilibrium position trajectory outpaced the low-pass dynamics of the pendulum. Therefore, the angle increased and the reaction torque became more negative, yielding large magnitude negative quasi-stiffness values. This highlights the ability of the quasi-stiffness measurements to obtain results that are not physically realizable with a mechanical spring or stable controller.

These observations also held true in our bipedal walking model—which is more analogous to human walking. The quasi-stiffness was zero at the beginning of the stance cycle and larger during late stance, which is consistent with the torque–angle relationship in human walking. This simulated behavior was caused by the time-varying equilibrium trajectory in the impedance controller. The actual ankle angle closely followed the equilibrium angle just after heel strike (resulting in no corrective torque), but tracking error grew as the equilibrium angle increased through the stance cycle (resulting in corrective torques). Therefore, the torque–angle relationship did not reflect the stiffness for the vast majority of the stance cycle.

Just as the quasi-stiffness appropriately influenced the design of passive prosthetic ankles, these simulations motivate the need to determine the stiffness or impedance of the able-bodied ankle during walking for biomimetic powered prosthesis control. That is, to accurately replicate the dynamics of the able-bodied ankle, we must have a thorough understanding of the underlying mechanics during walking. Such a biomimetic control system would likely be more intuitive for the user to wear and respond more appropriately on uneven terrains, where there are substantial unexpected changes to the ankles position. However, to estimate the ankle's impedance without knowledge of the equilibrium angle trajectory in a parametric impedance model, the ankle must be perturbed to identify its dynamics. Perturbations have been used to study ankle stiffness during static tasks, such as sitting [32] or supine lying [33]. Previously, researchers have determined ankle stiffness by applying angular or torque perturbations and analyzing the corresponding torque or position output [31], [34]–[37]. Since these studies focus on ankle stiffness during static tasks, they provide little insight into ankle stiffness during walking or other gait modalities. In order to determine ankle stiffness during the stance phase of walking, we have recently developed a platform robot capable of perturbing

the ankle about its center of rotation and measuring the reaction torque [38]. With a thorough understanding of the similarities and differences between stiffness and quasi-stiffness, future work can focus on the estimation of ankle and knee impedance during walking—thereby laying the foundation for biomimetic controller development for powered lower extremity prostheses.

REFERENCES

[1] A. H. Hansen, D. S. Childress, S. C. Miff, S. A. Gard, and K. P. Mesplay, "The human ankle during walking: Implications for design of biomimetic ankle prostheses," *J Biomech.*, vol. 37, no. 10, pp. 1467–1474, Oct. 2004.

[2] R. J. Butler, H. P. Crowell, and I. M. C. Davis, "Lower extremity stiffness: Implications for performance and injury," *Clin. Biomech.*, vol. 18, no. 6, pp. 511–517, 2003.

[3] M. L. Latash and V. M. Zatsiorsky, "Joint stiffness: Myth or reality?" *Human Movement Sci.*, vol. 12, pp. 653–692, 1993.

[4] S. Au and H. Herr, "On the design of a powered ankle-foot prosthesis: The Importance of series and parallel motor elasticity," *IEEE Robot. Autom. Mag.*, vol. 15, no. 3, pp. 52–59, Sep. 2008.

[5] D. A. Winter, "Energy generation and absorption at the ankle and knee during fast, natural, and slow cadences," *Clin. Orthopaedics Related Res.*, vol. 175, pp. 147–154, 1983.

[6] N. H. Molen, "Energy-speed relation of below-knee amputees walking on a motor-driven treadmill," *Int. Z Angew Physiol.*, vol. 31, no. 3, pp. 173–85, Mar. 2, 1973.

[7] E. G. Gonzalez, P. J. Corcoran, and R. L. Reyes, "Energy expenditure in below-knee amputees: Correlation with stump length," *Arch. Phys. Med. Rehabil.*, vol. 55, no. 3, pp. 111–119, Mar. 1974.

[8] M. J. Hsu, D. H. Nielsen, S. J. Lin-Chan, and D. Shurr, "The effects of prosthetic foot design on physiologic measurements, self-selected walking velocity, and physical activity in people with transtibial amputation," *Arch. Phys. Med. Rehabil.*, vol. 87, no. 1, pp. 123–129, Jan. 2006.

[9] T. R. Dillingham, L. E. Pezzin, and E. J. MacKenzie, "Limb amputation and limb deficiency: Epidemiology and recent trends in the United States," *South Med. J.*, vol. 95, no. 8, pp. 875–883, 2002.

[10] S. K. Au, J. Weber, and H. Herr, "Biomechanical design of a powered ankle-foot prosthesis," in *Proc. IEEE 10th Int. Conf. Rehabil. Robot.*, Jun. 2007, pp. 298–303.

[11] A. H. Hansen and D. S. Childress, "Effects of adding weight to the torso on roll-over characteristics of walking," *J. Rehabil. Res. Dev.*, vol. 42, no. 3, pp. 381–390, 2005.

[12] H. Houdijk, H. C. Doets, M. Van Middelkoop, and H. E. Dirkjan Veeger, "Joint stiffness of the ankle during walking after successful mobile-bearing total ankle replacement," *Gait Posture*, vol. 27, no. 1, pp. 115–119, 2008.

[13] C. T. Farley and D. C. Morgenroth, "Leg stiffness primarily depends on ankle stiffness during human hopping," *J Biomech*, vol. 32, no. 3, pp. 267–273, Mar. 1999.

[14] C. T. Farley, H. H. P. Houdijk, C. Van Strien, and M. Louie, "Mechanism of leg stiffness adjustment for hopping on surfaces of different stiffnesses," *J. Appl. Physiol.*, vol. 85, no. 3, pp. 1044–1055, 1998.

[15] S. D. Lark, J. G. Buckley, S. Bennett, D. Jones, and A. J. Sargeant, "Joint torques and dynamic joint stiffness in elderly and young men during stepping down," *Clin. Biomech.*, vol. 18, no. 9, pp. 848–855, 2003.

[16] H. Hobara, K. Kimura, K. Omuro, K. Gomi, T. Muraoka, S. Iso, and K. Kanosue, "Determinants of difference in leg stiffness between endurance-and power-trained athletes," *J. Biomech.*, vol. 41, no. 3, pp. 506–514, 2008.

[17] K. Shamaei, M. Cenciarini, and A. M. Dollar, "On the mechanics of the ankle in the stance phase of gait," in *Proc. Annu. Conf. IEEE Eng. Med. Biol. Soc.*, vol. 2011, pp. 8135–8140, 2011.

[18] R. B. Davis and P. A. DeLuca, "Gait characterization via dynamic joint stiffness," *Gait Posture*, vol. 4, no. 3, pp. 224–231, 1996.

[19] V. Dietz and T. Sinkjaer, "Spastic movement disorder: impaired reflex function and altered muscle mechanics," *Lancet Neurol.*, vol. 6, no. 8, pp. 725–733, Aug. 2007.

[20] D. A. Winter, A. E. Patla, F. Prince, M. Ishac, and K. Gielo-Perczak, "Stiffness control of balance in quiet standing," *J. Neurophysiol.*, vol. 80, no. 3, pp. 1211–1221, Sep. 1998.

[21] I. D. Loram and M. Lakie, "Direct measurement of human ankle stiffness during quiet standing: The intrinsic mechanical stiffness is insufficient for stability," *J. Physiol.*, vol. 545, no. 3, pp. 1041–1053, 2002.

[22] A. Goswami, B. Thuilot, and B. Espiau, "A study of the passive gait of a compass-like biped robot: Symmetry and chaos," *Int. J. Robot. Res.*, vol. 17, no. 12, pp. 1282–1301, Dec. 1998.

[23] R. D. Gregg, Y. Dhaher, A. Degani, and K. M. Lynch, "On the mechanics of functional asymmetry in bipedal walking," *IEEE Trans. Biomed. Eng.*, vol. 59, no. 5, pp. 1310–1318, May 2012.

[24] R. D. Gregg and J. W. Sensinger, "Towards biomimetic virtual constraint control of a powered prosthetic leg," *IEEE Trans. Control Syst. Technol.*, 2012, in press.

[25] R. M. Murray, Z. Li, and S. Sastry, *A Mathematical Introduction to Robotic Manipulation*. Boca Raton, FL: CRC Press, 1994.

[26] A. H. Hansen and D. S. Childress, "Investigations of roll-over shape: implications for design, alignment, and evaluation of ankle-foot prostheses and orthoses," *Disabil. Rehabil.*, vol. 32, no. 26, pp. 2201–2209, 2010.

[27] R. D. Gregg and J. W. Sensinger (2012). From machine to biomimetic control of powered prosthetic legs presented at the Dynamic Walking Conf., Pensacola, FL [Online]. Available: http://youtu.be/TZt0jSg5XSU

[28] P. de Leva, "Adjustments to Zatsiorsky–Seluyanov's segment inertia parameters," *J Biomech.*, vol. 29, no. 9, pp. 1223–1230, Sep. 1996.

[29] P. G. Adamczyk, S. H. Collins, and A. D. Kuo, "The advantages of a rolling foot in human walking," *J. Exp. Biol.*, vol. 209, no. Pt 20, pp. 3953–3963, Oct. 2006.

[30] E. J. Rouse, L. J. Hargrove, E. J. Perreault, and T. A. Kuiken, "Estimation of human ankle impedance during walking using the Perturberator robot," in *Proc. IEEE Int. Conf. Biomed. Rob. Biomechatronics*, 2012, pp. 373–378.

[31] P. L. Weiss, I. W. Hunter, and R. E. Kearney, "Human ankle joint stiffness over the full range of muscle activation levels," *J. Biomech.*, vol. 21, no. 7, pp. 539–544, 1988.

[32] T. Sinkjaer, E. Toft, S. Andreassen, and B. C. Hornemann, "Muscle stiffness in human ankle dorsiflexors: Intrinsic and reflex components," *J. Neurophysiol.*, vol. 60, no. 3, pp. 1110–1121, Sep. 1988.

[33] R. E. Kearney, R. B. Stein, and L. Parameswaran, "Identification of intrinsic and reflex contributions to human ankle stiffness dynamics," *IEEE Trans. Biomed. Eng.*, vol. 44, no. 6, pp. 493–504, Jun. 1997.

[34] A. Roy, H. I. Krebs, C. T. Bever, L. W. Forrester, R. F. Macko, and N. Hogan, "Measurement of passive ankle stiffness in subjects with chronic hemiparesis using a novel ankle robot," *J. Neurophysiol.*, vol. 105, no. 5, pp. 2132–2149, 2011.

[35] R. E. Kearney and I. W. Hunter, "Dynamics of human ankle stiffness: Variation with displacement amplitude," *J. Biomech.*, vol. 15, no. 10, pp. 753–756, 1982.

[36] R. E. Kearney and I. W. Hunter, "System identification of human joint dynamics," *Crit. Rev. Biomed. Eng.*, vol. 18, no. 1, pp. 55–87, 1990.

[37] M. M. Mirbagheri, H. Barbeau, and R. E. Kearney, "Intrinsic and reflex contributions to human ankle stiffness: Variation with activation level and position," *Exp. Brain Res.*, vol. 135, no. 4, pp. 423–436, Dec. 2000.

[38] E. J. Rouse, L. J. Hargrove, M. A. Peshkin, and T. A. Kuiken, "Design and validation of a platform robot for determination of ankle impedance during ambulation," in *Proc. Int. Conf. IEEE Eng. Med. Biol. Soc.*, Aug. 2011, vol. 2011, pp. 8179–8182.

Elliott J. Rouse (S'10–M'12) received the B.S. degree in mechanical engineering from the Ohio State University, Columbus, in 2007, and the M.S. and Ph.D. degrees in biomedical engineering from Northwestern University, Evanston, IL, in 2009 and 2012, respectively.

He is currently a Postdoctoral Associate in the Biomechatronics Group, MIT Media Lab, Cambridge, MA, where he is involved in the development of novel robotic prosthetic technologies. His main research interests include wearable robotics, biomedical system dynamics and identification, medical device design, optimization theory, and culminating in the development of technologies to assist and augment human function.

Robert D. Gregg (S'08–M'10) received the B.S. degree in electrical engineering and computer sciences from the University of California, Berkeley, in 2006, and the M.S. and Ph.D. degrees in electrical and computer engineering from the University of Illinois at Urbana-Champaign, Urbana, in 2007 and 2010, respectively.

He is currently a Research Scientist at the Center for Bionic Medicine, Rehabilitation Institute of Chicago, Chicago, IL, and an Engineering into Medicine Fellow in the Department of Mechanical Engineering, Northwestern University, Evanston, IL. His research is focused on control mechanisms of bipedal locomotion with application to both autonomous and wearable robots.

Dr. Gregg received a Career Award at the Scientific Interface from the Burroughs Wellcome Fund. He also received the Best Technical Paper Award of the 2011 International Conference on Climbing and Walking Robots, the 2009 O. Hugo Schuck Award from the International Federation of Automatic Control American Automatic Control Council, and the Best Student Paper Award of the 2008 American Control Conference.

Levi J. Hargrove (S'05–M'08) received the B.Sc.,M.Sc., and Ph.D. degrees in electrical engineering from the University of New Brunswick, Fredericton, NB, Canada, in 2003, 2005, and 2007, respectively.

In 2008, he joined the Center for Bionic Medicine at the Rehabilitation Institute of Chicago, Chicago, IL. He is also a Research Assistant Professor in the Department of Physical Medicine and Rehabilitation and Biomedical Engineering, Northwestern University. Evanston, IL. His research interests include pattern recognition, biological signal processing, and myoelectric control of powered prostheses.

Dr. Hargrove is a member of the Association of Professional Engineers and Geoscientists of New Brunswick.

Jonathon W. Sensinger (M'09) received the B.S. degree in bioengineering from the University of Illinois at Chicago, Chicago, in 2002, and the Ph.D. degree in biomedical engineering from Northwestern University, Chicago, IL, in 2007.

He is the Director of the Prosthesis Design and Control Laboratory, Center for Bionic Medicine, Rehabilitation Institute of Chicago, Chicago, and a Research Assistant Professor at Northwestern University. His research interests include myoelectric and body-powered prosthesis interface control and mechatronic design.